crystals

MDPI

Article

Effects of Highly Crystalized Nano C-S-H Particles on Performances of Portland Cement Paste and Its Mechanism

Yuli Wang [1], Huijuan Lu [1], Junjie Wang [2,*] and Hang He [1]

[1] School of Materials Science and Engineering, Henan Polytechnic University, Jiaozuo 454003, China; wangyuli@hpu.edu.cn (Y.W.); 211906020051@home.hpu.edu.cn (H.L.); 211606020018@home.hpu.edu.cn (H.H.)

[2] Department of Civil Engineering, Tsinghua University, Beijing 100084, China

* Correspondence: junjiewang@tsinghua.edu.cn

Received: 28 July 2020; Accepted: 7 September 2020; Published: 15 September 2020

Abstract: In order to improve the early age strength of ordinary Portland cement-based materials, many early strength agents were applied in different conditions. Different from previous research, the nano calcium silicate hydrate (C-S-H) particles used in this study were synthesized through the chemical reaction of CaO, SiO_2, and H_2O under 120 °C using the hydrothermal method, and the prepared nano C-S-H particles were highly crystalized. The influences of different amounts of nano C-S-H particles (0%, 0.5%, 1%, 2% and 3% by weight of cement) on the setting time, compressive strength, and hydration heat of cement paste were studied. The hydration products and microstructure of the cement paste with different additions of nano C-S-H particles were investigated through thermogravimetry-differential thermal analysis (TG-DTA), X-ray powder diffraction (XRD), and scanning electron microscope (SEM) tests. The results show that the nano C-S-H particles could be used as an early strength agent, and the early strength of cement paste can be increased by up to 43% through accelerating the hydration of tricalcium silicate (C_3S). However, the addition of more than 2% nano C-S-H particles was unfavorable to the later strength development due to more space being left during the initial accelerated hydration process. It is suggested that the suitable content of the nano C-S-H particles is 0.5%−1% by weight of cement.

Keywords: highly crystalized nano C-S-H; early strength agent; setting time; compressive strength; microstructure

1. Introduction

Additives, such as rapid setting agents and early strength agents, have been widely used in various applications of cement and concrete in different projects. Early strength agents are needed for the projects that require a rapid development of early age strength—for example, when the environmental temperature is low, and when the quick repairing and reinforcement work using cementitious materials are required [1].

The most frequently used early strength agents in concrete can be divided into inorganic, organic, and complexing agents. The inorganic early strength agents are mainly chloride salts, sulfate salts, and nitrate salts [2]. Hoang-Anh Nguyen et al. [3] reported that the sodium sulfate accelerated the early hydration rate and strength of slag cement paste. They also showed that the pore structure of concrete was refined and modified, and the crack resistance of the concrete at the early age was increased by adding sodium sulfate. P. Carballosa et al. [4] found that the addition of expansive calcium sulfoaluminate agent could shorten the setting time of self-compacting concretes and modify the early age physical properties. Heesup et al. [5] reported that the nitrate salts and nitrite salts could increase

the early age strength of concrete by accelerating the hydration of C_3S and tricalcium aluminate (C_3A), and they could also promote the formation of nitrate and nitrite hydrates and the ettringite (AFt) at the early age. Although chloride salts could accelerate the hydration of cement paste, they also bring chloride ions, which can cause the corrosion of steel in concrete [6–10]. Other early strength agents containing potassium and sodium salts could cause the alkali silica reaction [11]. The common organic early strength agents are diethanolamine, triethanolamine, triethanolamine, and some organic salts, such as formate, acetate, etc. Triethanolamine is the most commonly used one. Triethanolamine can accelerate the hydration of C_3S in the induction period of cement hydration, and it has a positive impact on the later strength as well as increasing the early strength [12]. However, it is not suitable to use an organic agent such as triethanolamine for steam-curing concrete [13]. Complexing agents instead of a single agent could be used to modify any adverse effects caused by individual agents [14]. For example, Xiao et al. [15] reported that the combination of $C_6H_{15}O_3N$, $Al_2(SO_4)_3$, and Li_2CO_3 could increase the early age compressive strength of mortar by more than 200% without compromising other properties.

As the development of nanotechnology has accelerated in recent years, nanoparticles such as nano SiO_2 [16–19], $CaCO_3$ [20,21], TiO_2 [22], graphene oxide [23,24], core/shell TiO_2@SiO_2 [25], carbon nanotubes [26–32], and nano calcium silicate hydrate (C-S-H) [33,34] have been used in concrete. Wang et al. [20] showed that the addition of nano $CaCO_3$ particles could improve the mechanical properties of plain cement paste and modify the microstructure. Musso et al. [32] reported that adding 0.5% (by weight of cement) of multi-wall carbon nanotubes could improve the mechanical strength of plain cement paste, and the treatments on the carbon nanotubes by temperature annealing and acid oxidative were able to enhance this effect. Jee et al. [35] found that the addition of 0.5% (by weight of cement) of titanium nanotubes could increase the compressive strength of cement paste by 12% and the flexural strength by 23% even at the later age, and they reported that the nanotubes were able to fill the nanopores and bridge the microcracks in cement paste. It was reported [36] that the addition of silica nanoparticles could increase the mechanical and durability of concrete by filling the cement pores and reacting with $Ca(OH)_2$ to form additional C-S-H gel. Land and Stephan [37] found the main influencing factors of C-S-H seed as an early strength agent of cement were chemical composition and particle size, when they studied the effect of xonotlite and wollastonite C-S-H on the hydration and hardening of cement. Compared with nano SiO_2, the influence of nano C-S-H is more obvious on the development of strength at age from the first day [34]. Meanwhile, nano SiO_2 has pozzolanic reactivity, and nano C-S-H has filling and nucleation effects.

Since the main hydration product in ordinary Portland cement paste is C-S-H gel, some studies have reported the effect of nano C-S-H particles on the hydration of cement paste. For example, it was presented [38] that nano C-S-H can accelerate cement hydration and improve its early compressive strength. Deyu Kong [39] found that nano C-S-H gel can mitigate the retardation caused by the sucrose. Kanchanason and Plank [40] synthesized nano C-S-H and polycarboxylate (PCE) comb polymer suspension, and they found that this suspension (solid content equals 2% by weight of cement) could accelerate the hydration of slag and calcined clay blended cements and increase the compressive strength by 240% after 16 h of hydration compared to the control groups. Wang et al. [38] synthesized nano C-S-H together with polycarboxylate (PCE) and polysulfonate (PSE), which were applied as stabilizer, and they found that the induction period of cement could be clearly shortened. Meanwhile, the specimen with PCE-type C-S-H showed a more obvious boosting effect than that with PSE type C-S-H. Das et al. [41] synthesized C-S-H nanocrystals by chemical reaction using bagasse as raw material, and they found that adding C-S-H seeds in concrete can accelerate the hydration process of cement within one day and increase the early strength by 30–50%, but it does not affect the later compressive strength.

Almost all reported references mainly focused on the effect that amorphous state C-S-H seeds had on the hydration of cement, but the highly crystalized C-S-H particles were rarely reported elsewhere. The reason highly crystalized C-S-H particles were used was that the existence of C-S-H in nature

was mostly found in crystalized form. In addition, the action mechanism of nano C-S-H remains unclear [19]. Investigations on the influence of highly crystalized nano C-S-H particles as an early strength agent on the hydration of cement paste with the addition of 0%, 0.5%, 1%, 2%, and 3% nano C-S-H particles (by weight of cement) were conducted through a series of tests including setting time, compressive strength, hydration heat, TG-DTA, XRD, and SEM. The results are analyzed and discussed, and a suggestion for the optimum content of the nano C-S-H particles is put forward.

2. Materials and Methods

2.1. Materials

2.1.1. Cement

Type I Portland cement P.O. 42.5 confirming to GB 175−2007 [42] was used in this study. The main properties and chemical compositions of the cement are shown in Tables 1 and 2.

Table 1. Properties of Cement

Fineness/%	Stability	Setting Time/min		Flexural Strength/MPa		Compressive Strength/MPa	
		Initial	Final	3 Days	28 Days	3 Days	28 Days
1.6	Satisfied	169	356	5.9	9.7	32.2	51.4

Table 2. Chemical composition of Cement/%

SiO_2	CaO	Al_2O_3	Fe_2O_3	MgO	Na_2O	K_2O	LOI
23.81	62.01	5.39	3.18	2.92	0.29	0.16	0.15

2.1.2. Synthesis of Nano C-S-H

The nano C-S-H suspension was synthesized through the hydrothermal method [43,44] shown in Figure 1. Calcium oxide (CaO, chemical purity more than 99.99%) and fumed silica (SiO_2) were mixed together with a molar ratio of 1:1. The mixed powders were put into an autoclave. De-ionized water was added into the autoclave with water/solids (mass ratio) at 10:1. The powders and water were mixed together for 5 min to form a suspension. The temperature inside the autoclave was maintained at 120 °C for 6 h with a stirring speed of 400 rpm to allow the reaction among CaO, SiO_2, and H_2O to form C-S-H. Then, the attained nano C-S-H suspension was allowed to cool down naturally to room temperature and sealed to avoid any further evaporation or carbonation. Meanwhile, nano C-S-H was dried in vacuum at 60 °C. The measured solid content in the nano C-S-H suspension was 22%. Figure 2a shows the particle size distribution by laser diffraction of the nano C-S-H particles from the suspension, and it can be seen that the particle size of the nano C-S-H particles ranges from 80 to 600 nm. Figure 2b shows the XRD pattern of the nano C-S-H particles, and the peaks show that the mineral phases in the nano C-S-H particles are mainly tobermorite and jennite, which agrees well with previous literature [45,46], and there are also traces of SiO_2 and wollastonite. Figure 2c shows the SEM image of synthesized nano C-S-H particles, and the image shows that the shape of nano C-S-H particles is polygon and the size is consistent with the results in Figure 2a.

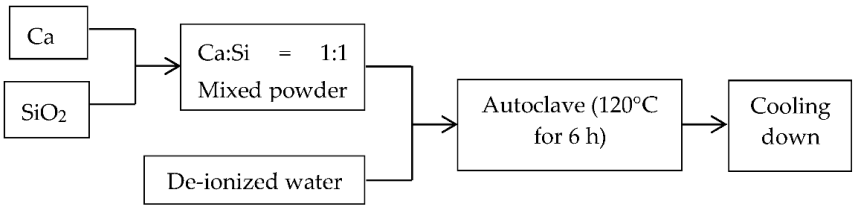

Figure 1. Scheme of the synthetic procedure of highly crystalized nano calcium silicate hydrate (C-S-H) particles.

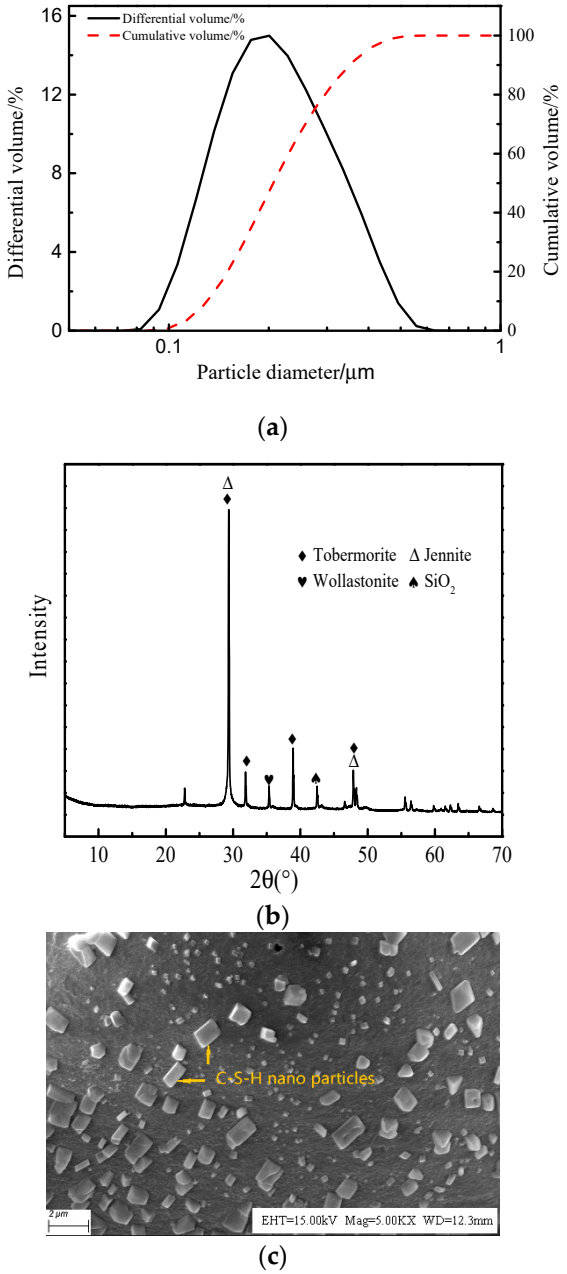

Figure 2. (**a**) Particle distribution of synthesized nano C-S-H particles; (**b**) XRD pattern of the synthesized nano C-S-H particles; (**c**) SEM image of synthesized nano C-S-H particles.

2.1.3. Water

The mixing water for cement paste used was the normal tap water confirming to JGJ 63-2006 [47].

2.2. *Sample Preparation*

The water–cement ratio was kept constant as 0.4. The nano C-S-H particles (0%, 0.5%, 1%, 2%, and 3% by weight of cement) were considered as the additional additive. The water content in the nano C-S-H suspension was considered as a part of the mixing water. The mixing procedure is as follows: the nano C-S-H suspension was treated with ultrasonic sonication for 5 min before mixing, the required amount of nano C-S-H suspension was mixed together with the additional water first; then, cement powder was added in a mixer bowl, and the mixed suspension was added and mixed together with the cement powder at a speed of 120 rpm for 5 min using the automatic mixer. Then, the

fresh paste was transferred into 40 mm × 40 mm × 40 mm molds. All samples were demolded after 24 h and stored in a standard curing room (20 °C, 97% relative humidity (R.H.)) until further tests.

2.3. Methods

2.3.1. Setting Time

The initial and final setting times of cement paste were tested according to GB/T1346-2011 [48].

2.3.2. Compressive Strength

The compressive strength of cement paste (40 mm × 40 mm × 40 mm) was tested by the same loading procedure as described in GB/T17671-1999 [49]. The tests were conducted at the age of 1, 7, and 28 days. Each group was measured three times, and then the average value was taken.

2.3.3. Hydration Heat

A multichannel thermal activity monitor (TAM) air micro calorimeter was used for the hydration heat monitoring. The chamber was stabilized for 0.5 h to achieve a table temperature of 20 °C before the isothermal test was started, and the test lasted for 72 h.

2.3.4. XRD

The same powder sample as the TG-DTA test was used for XRD. An X-ray diffractometer of Rigaku SmartLab was used for the measurements. The test voltage was 40 kV, and the working current was 150 mA. The scanning was from 5° to 70° at a rate of 10°/min.

2.3.5. TG-DTA

After the compression tests, representative pieces of the samples from the inner part of the cubic paste sample were immersed into absolute ethyl alcohol for 24 h to stop the hydration [50]. Then, the pieces were dried in a vacuum oven at 60 °C for 24 h [51], followed by grounding into powder passing a sieve of 75 μm. TG-DTA tests were conducted in a simultaneous thermal analyzer in an N_2 environment, and the heating temperature was from 20 to 900 °C by a heating rate of 10 °C/min.

2.3.6. SEM

The piece samples after the termination of hydration and vacuum drying were used for SEM observation. Samples were gold coated, and the observations were conducted under high vacuum conditions.

3. Results and Discussion

3.1. Influence of Nano C-S-H on the Setting Time of Cement Paste

Results of the effect of different contents of nano C-S-H particles on the initial and final setting times of the cement paste are shown in Figure 3. It can be seen that both the initial and final setting times were shortened with the addition of nano C-S-H particles. Compared to the sample without nano C-S-H particles, the initial setting time was decreased by 7%, 12%, 19%, and 26% for the pastes with 0.5%, 1%, 2%, and 3% of nano C-S-H, respectively; and the final setting time was decreased by 6%, 13%, 23%, and 30% for the pastes with 0.5%, 1%, 2%, and 3% of nano C-S-H, respectively. Similar as the seeding effect of amorphous C-S-H particles, this effect could be mainly caused by the seeding effect [38,39] of the nanoparticles, which accelerated the initial hydration of cement. This was consistent with previous research results [41,52].

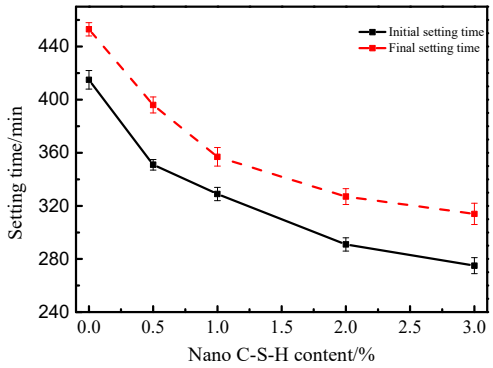

Figure 3. The initial and final setting times of cement paste with different contents of nano C-S-H particles.

3.2. Influence of Nano C-S-H on the Compressive Strength of Cement Paste

Figure 4 shows the results of the compressive strength at the age of 1, 7, and 28 days of the cement paste samples with addition of 0%, 0.5%, 1%, 2%, and 3% nano C-S-H. The average compressive strength of the cement paste with no nano C-S-H addition are 16.7, 44.1, and 66.8 MPa at the age of 1, 7, and 28 days, respectively. Compared to the strength results of the paste with no nano C-S-H addition, both of the compressive strength results at the age of 1 and 7 days were improved, but the strength results at the age of 28 days were decreased. Specifically, the compressive strength at the age of 1 day was increased by 6%, 7%, 25%, and 43%, and the compressive strength at the age of 7 days was increased by 10%, 11%, 19%, and 14% in the samples with the additions of 0.5%, 1%, 2%, and 3% nano C-S-H particles, respectively. This is consistent with the previous research results [34,50]. At the age of 28 days, the compressive strength was decreased by 3%, 5%, 13%, and 14% in the cement paste with the addition of 0.5%, 1%, 2%, and 3% nano C-S-H particles, respectively, when compared to the paste sample with no nano C-S-H addition.

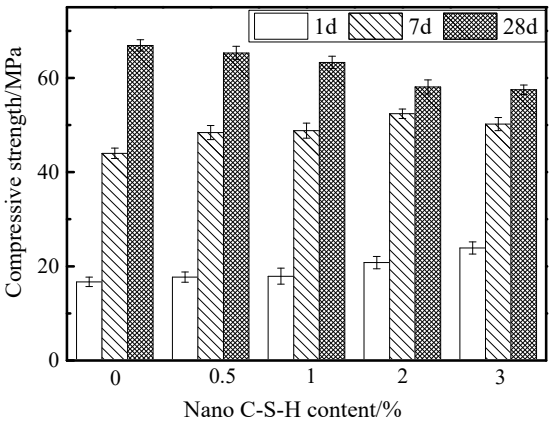

Figure 4. Compressive strength of cement pastes with the addition of different contents of nano C-S-H at the age of 1, 7, and 28 days.

It is indicated the nano C-S-H particles accelerated the early age hydration of cement paste and increased the early age compressive strength (1 and 7 days). The reason for the decrease of the compressive strength at 28 days could be attributed to the acceleration effect caused by nano C-S-H particles becoming insignificant and disappearing after the first few days [39]. The initial rapid accumulation of hydration products around the nano C-S-H particles could leave some defects, which is harmful for the long-term strength development; this will be further verified by SEM observations.

In consideration of the compressive strength at all the 3 tested ages (1, 7, and 28 days), the content of nano C-S-H particles should be no more than 1% by weight of cement, given that it could improve the early age strength without significantly compromising the later age strength.

3.3. Hydration Heat Results

Figure 5 shows the hydration heat rate results of the cement paste samples with the addition of different contents of nano C-S-H particles. There are two main peaks on the curves of the hydration heat, namely here the first and second peaks. The first peak happened at around 1.8 min, and the second one happened between 12 and 18 h. The first peak was mainly because of the dissolution of cement powder and formation of AFt [51], and the second peak was mainly because of the hydration of C_3S in the cement.

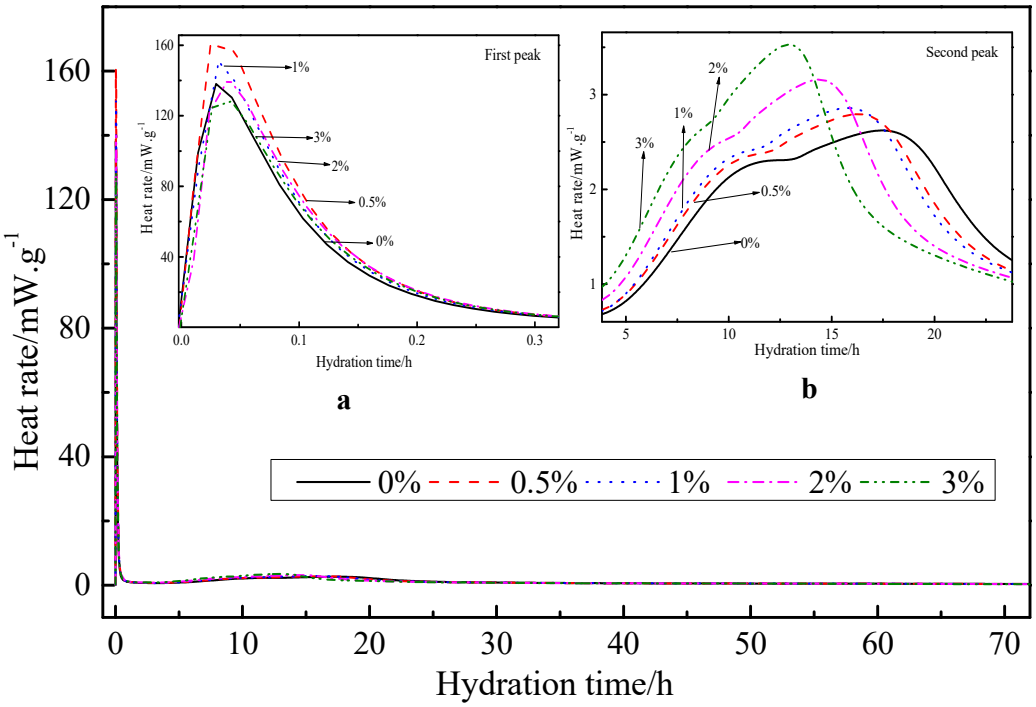

Figure 5. Hydration heat rate of cement paste with different amounts of nano C-S-H addition.

At the location of the first peak, the mixes with the addition of nano C-S-H particles showed an overall higher peak heat rate than that with no nano C-S-H. It is suggested that the addition of nano C-S-H contributed to a better dispersion effect of the cement powder. Wang et al. [33] also found that the addition of low-dose nano C-S-H significantly shortened the induction period and increased the height of the peak hydration rate. The hydration exothermic rate of cement with 0.5% nano C-S-H is slightly higher than that with 1% nano C-S-H. As for the second peak, it can be clearly seen that the peak heat rate was higher in the mix with a higher content of nano C-S-H particles, and the peak time was also earlier in the mix with a higher content of nano C-S-H particles. Specifically, the heat rate of second peak for the mixes with 0%, 0.5%, 1%, 2%, and 3% were 2.62, 2.79, 2.87, 3.16, and 3.54 mW/g, respectively; and the related peak time was 17.62, 16.28, 15.83, 14.57, and 12.96 h. Meanwhile, the accumulated heat generated of this period is shown in Table 3. The results show that the nano C-S-H particles obviously accelerated the hydration of C_3S and promoted the formation of new C-S-H. This effect was more obvious when a higher content of nano C-S-H particles was added. The nano C-S-H particles act as nucleation centers and dispersing agents in cement paste. Due to the unique characteristics of nanoparticles, the hydration process is accelerated, including the increase of hydration rate peak and the decrease of induction period [53].

Table 3. Results of Accumulated Hydration Heat.

Nano C-S-H Content/%	MHR/mW g^{-1}	AHH at MHR/J g^{-1}	1 d AHH/J g^{-1}	3 d AHH/J g^{-1}
0	2.62	179	228	345
0.5	2.79	184	244	359
1	2.87	178	239	355
2	3.16	177	246	360
3	3.54	169	250	361

Note: AHH—accumulated hydration heat, MHR—maximum heat rate.

Figure 6 shows the accumulated heat generated in each mix, and the results indicate that the mixes with the addition of nano C-S-H particles showed a higher accumulated hydration heat than those without nano C-S-H particles. The mix with a higher content of nano C-S-H particles generally shows a higher accumulated hydration heat. In 1 day, as can be seen from Figure 6b and Table 3, nano C-S-H can increase the hydration heat of Portland cement. The results of the accumulated heat generated in cement pastes were consistent with the development of compressive strength. It is indicated that nano C-S-H particles obviously accelerated the hydration of ordinary Portland cement powders and increased the hydration heat. It is interesting to see that the accumulated heat at 3 days is very similar for 0.5%, 1.0%, 2.0%, and 3.0% mixes. By comparing with the data of 1 day, it could be indicated that nano C-S-H mainly promoted the hydration of cement in 1 day, but it has no obvious effect on the total accumulated heat at the later stage after 3 days.

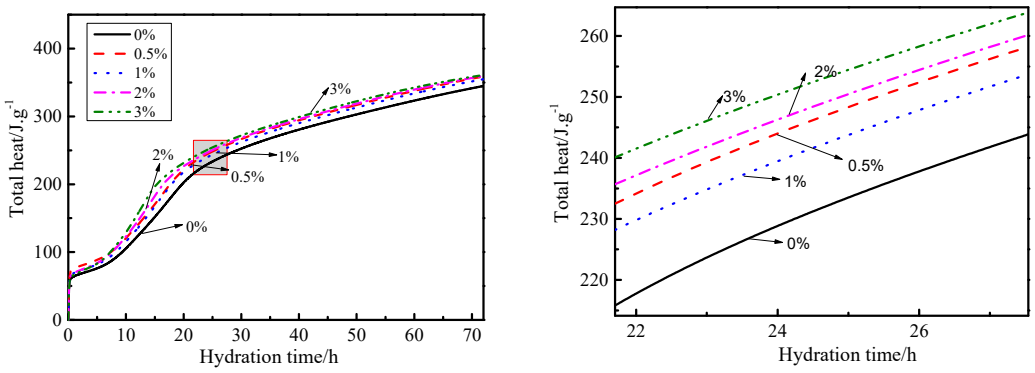

Figure 6. (**a**) Accumulated hydration heat of cement paste with different amounts of nano C-S-H addition; (**b**) Local enlarged view.

3.4. XRD Results

Figure 7 shows the XRD results of the cement paste samples with different contents (0%, 0.5%, 1%, 2%, and 3%) of nano C-S-H particles at the different ages: 1, 7, and 28 days. The main phase compositions in the cement paste samples reflected by XRD spectrum are $Ca(OH)_2$, $CaCO_3$, AFt, AFm, C_2S, and C_3S [51] As stated earlier, the formation of $CaCO_3$ could be due to the CO_2 dissolved in mixing water, and the AFm here is CO_2-AFm. At the age of 1 day, the peak height of AFt firstly increased and then decreased when the content of nano C-S-H particles increased from 0 to 3%; the highest peak happened in the mix with 1% nano C-S-H particles. This was consistent with the results of quantitative analysis by Zhang et al [34]. These results suggest that the addition of nano C-S-H particles facilitated the formation of $Ca(OH)_2$ and AFt. It should be noted that the comparison between peak heights does not actually give the precise quantitative analysis. It should be more precise to perform Rietveld analysis to quantify the amount of the different phases.

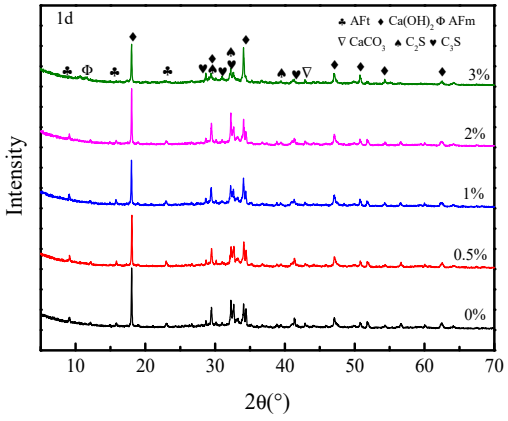

(**a**) 1 d.

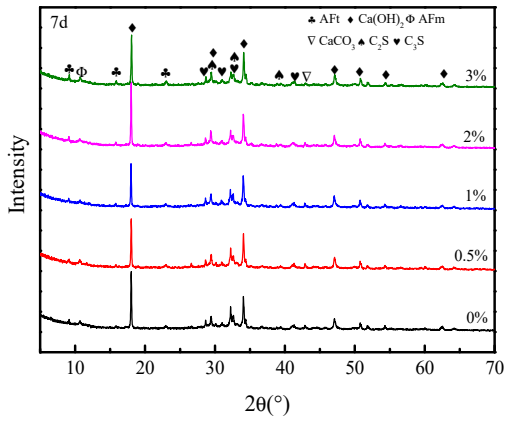

(**b**) 7 d.

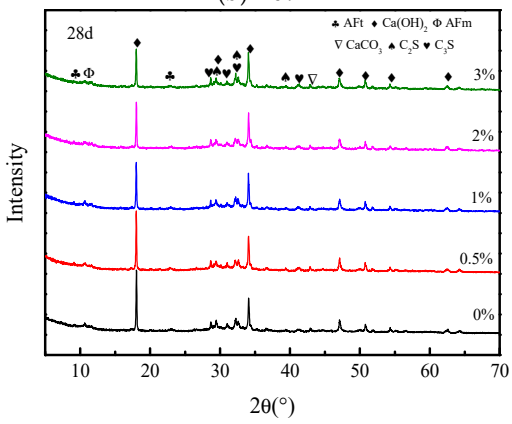

(**c**) 28 d

Figure 7. XRD powder diffraction patterns of the sample with different contents of nano C-S-H particles at the age of 1, 7, and 28 days.

The changing patterns of the phase compositions at the age of 7 days are similar to those at 1 day. In the presence of C-S-H, the existence of a high peak value indicated a greater precipitation of hydration products [53], which could improve the microstructure and compressive strength of cement paste. The XRD result was consistent with that of compressive strength. With the increase of hydration time, the content of AFt first increases and then decreases, due to the transformation of AFt into AFm after the depletion of the sulfate phase, which was most obvious at 28 days of age.

3.5. TG-DTA Results

Figure 8 shows the TG-DTA results of the different paste samples with 0%, 0.5%, 1%, 2%, and 3% nano C-S-H particles at the age of 1, 7, and 28 days. There are 3 main peaks on the DTA curves: the first peak is at around 110 °C, which is the weight loss of water from AFt and C-S-H [51]; the second peak is at around 460 °C which is the decomposition of $Ca(OH)_2$; and the third peak is at around 700 °C which is the decomposition of $CaCO_3$. Additionally, there is a small peak at around 160 °C which is the water loss from the AFm (CO_2-AFm) [21].

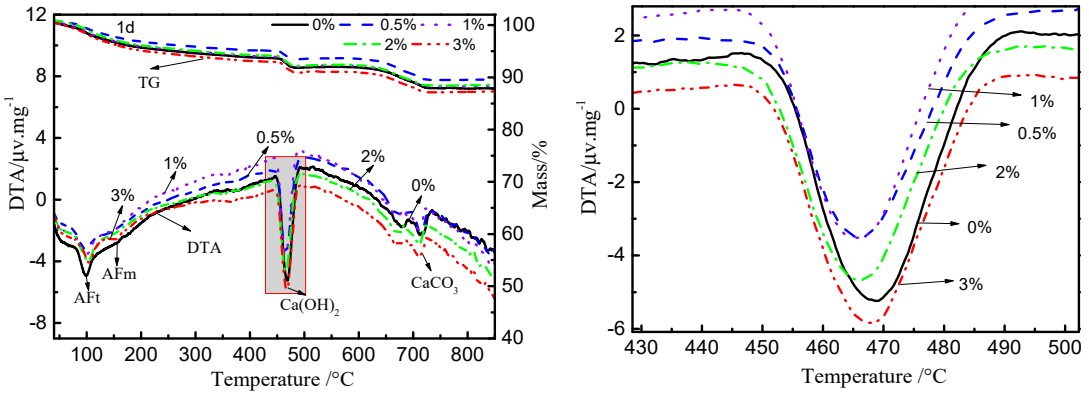

(**a**) 1 d.

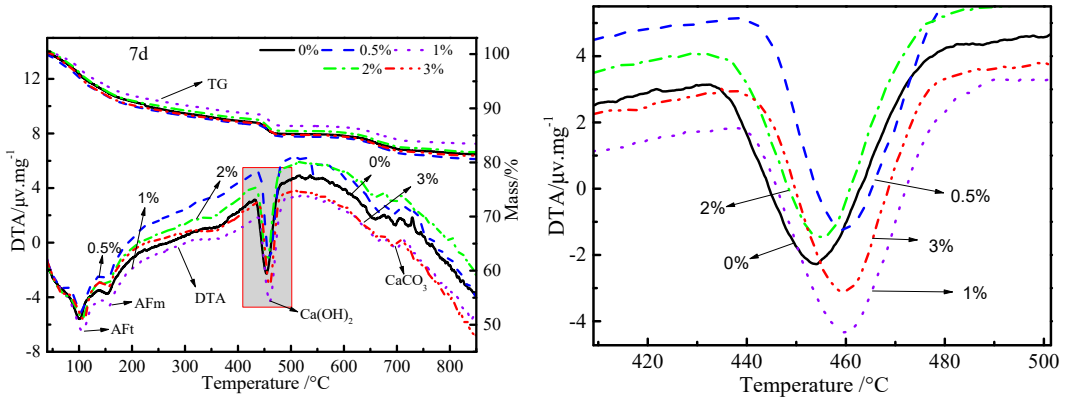

(**b**) 7 d.

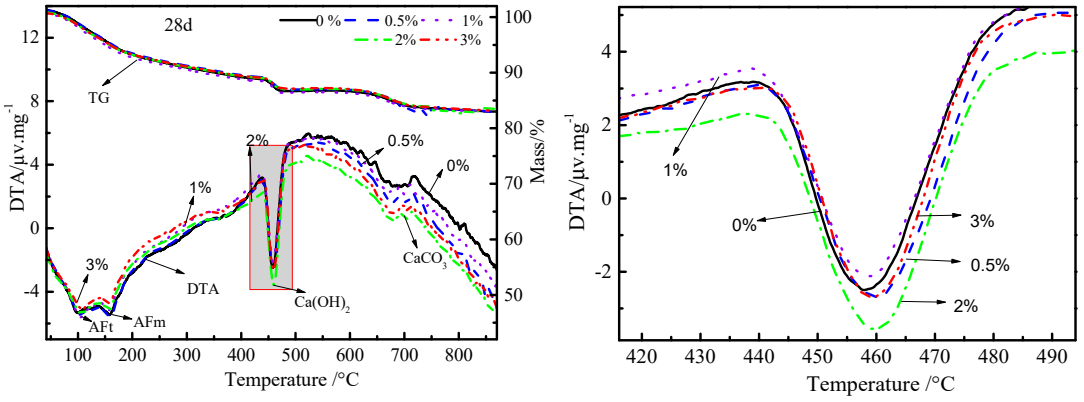

(**c**) 28 d.

Figure 8. Thermogravimetry-differential thermal analysis (TG-DTA) results of cement paste with different contents of nano C-S-H at the age of 1, 7, and 28 days; the sub-figure on the right was a local enlarged view of the peak of $Ca(OH)_2$ on the left.

At the age of 1 day, the weight losses at the location of the first peak for the paste samples with 0%, 0.5%, 1%, 2%, and 3% nano C-S-H particles were 5.8%, 5.9%, 6.0%, 5.0%, and 5.1%; the weight losses at the location of $Ca(OH)_2$ based on a tangential model for the paste samples with 0%, 0.5%, 1%, 2%, and 3% nano C-S-H particles were 1.73%, 1.57%, 1.75%, 1.77%, and 2.04%, respectively, as shown in Table 4. At the age of 7 days, the weight losses at the location of the first peak for the paste samples with 0%, 0.5%, 1%, 2%, and 3% nano C-S-H particles were 6.7%, 7.0%, 6.5%, 6.0%, and 5.7%; the weight losses at the location of $Ca(OH)_2$ for the paste samples with 0%, 0.5%, 1%, 2%, and 3% nano C-S-H particles were 1.87%, 1.98%, 2.07%, 1.94%, and 1.98%, respectively. At the age of 28 days, the weight losses at the location of the first peak (4.6%) and location of $Ca(OH)_2$ (2.0%) were almost the same for different paste samples, since that their TG curves were similar to each other. The weight loss rate in TG curves is consistent with that in the DTA diagram. These results show that at the early ages (1 and 7 days), the nano C-S-H particles accelerated the formation of $Ca(OH)_2$, which is the hydration product from C_3S at early age. As it is known that the formation of $Ca(OH)_2$ is associated with the new C-S-H gel, the nano C-S-H particles also promoted the formation of C-S-H gel. At the later age (28 days), the effect of nano C-S-H particles on the hydration products is not very significant. From the compressive strength results at 28 days, it can be seen that the different strength results could be caused by the different layout structure of the hydration products in different mixes [51] from 7 to 28 days, the consumption of $Ca(OH)_2$ was higher in the mixes with nano C-S-H particles.

Table 4. The Weight Loss of Ca(OH)2 at Different Ages.

Nano C-S-H/%	1 d Weight Loss/%	7 d Weight Loss/%	28 d Weight Loss/%
0	1.73	1.87	2.00
0.5	1.57	1.98	2.08
1	1.75	2.07	2.00
2	1.77	1.94	1.95
3	2.04	1.98	1.84

3.6. SEM Results

Figure 9 shows the images of the SEM observations at different ages (1, 7, and 28 days) for the cement pastes with the addition of different contents (0%, 0.5%, 1%, 2%, and 3%) of nano C-S-H particles. The hexagonal plates are $Ca(OH)_2$, the needle-shaped hydration products are AFt, and the gel in irregular shape is the C-S-H gel. It is difficult to find the previously added nano C-S-H particles, which could be wrapped with the newly formed C-S-H gel. Wang et al. [33] reported C-S-H gel is a substance that grows on nano C-S-H particles, and fibrous C-S-H was found at the age of 1 and 7 days; the content increased first and then decreased. At the age of 1 and 7 days (Figure 9a,b), $Ca(OH)_2$ is more commonly found in the cement pastes with the previously added nano C-S-H particles compared to the control group with no nano C-S-H addition. This phenomenon was not found at the age of 28 days. This should not be caused by the carbonation, since the sampling location is from the center part. Meanwhile, the pore size of needle-like material with nano C-S-H content of 0.5% and 1% is smaller than others, at about 3 μm.

When comparing the 28-days results of the compressive strength, XRD, TG-DTA, and the SEM images, it is indicated that the continuous decrease of the compressive strength of the cement paste with the increase of nano C-S-H additions is not caused by the overall amount of hydration products, which is similar in different mixes at 28 days based on the confirmation from the TG-DTA results, but it could be due to the microstructure of these hydration products. From Figure 9c, it can be seen that the microstructure of the hydration products in the mixes with the previous addition of nano C-S-H particles is less compact compared to the paste with no nano C-S-H additions, and the reason could be that the initial rapid accumulation of $Ca(OH)_2$ and new C-S-H gels around the added nano C-S-H particles left more unfavorable spaces, which could facilitate the development and propagation of microcracks. In addition, the later higher consumption rate of $Ca(OH)_2$ from 7 to 28 days in the

mixes with nano C-S-H additions could leave more frail spaces, which could also compromise the compressive strength. Some studies [34,54] reported that the addition of nano C-S-H nucleating agent actually increased the gel pores, the formed C-S-H from the nucleation of nano C-S-H was loosely packed, and the porosity of the hydration products was increased with the amount of nano-C-S-H crystal seeds. These agree with our finding that the addition of a higher content of nucleating agents makes the C-S-H gel structure become more porous at the later age. So, when there is too much nano C-S-H content, this may cause adverse reactions at the later age, which corresponds well to the results in this paper.

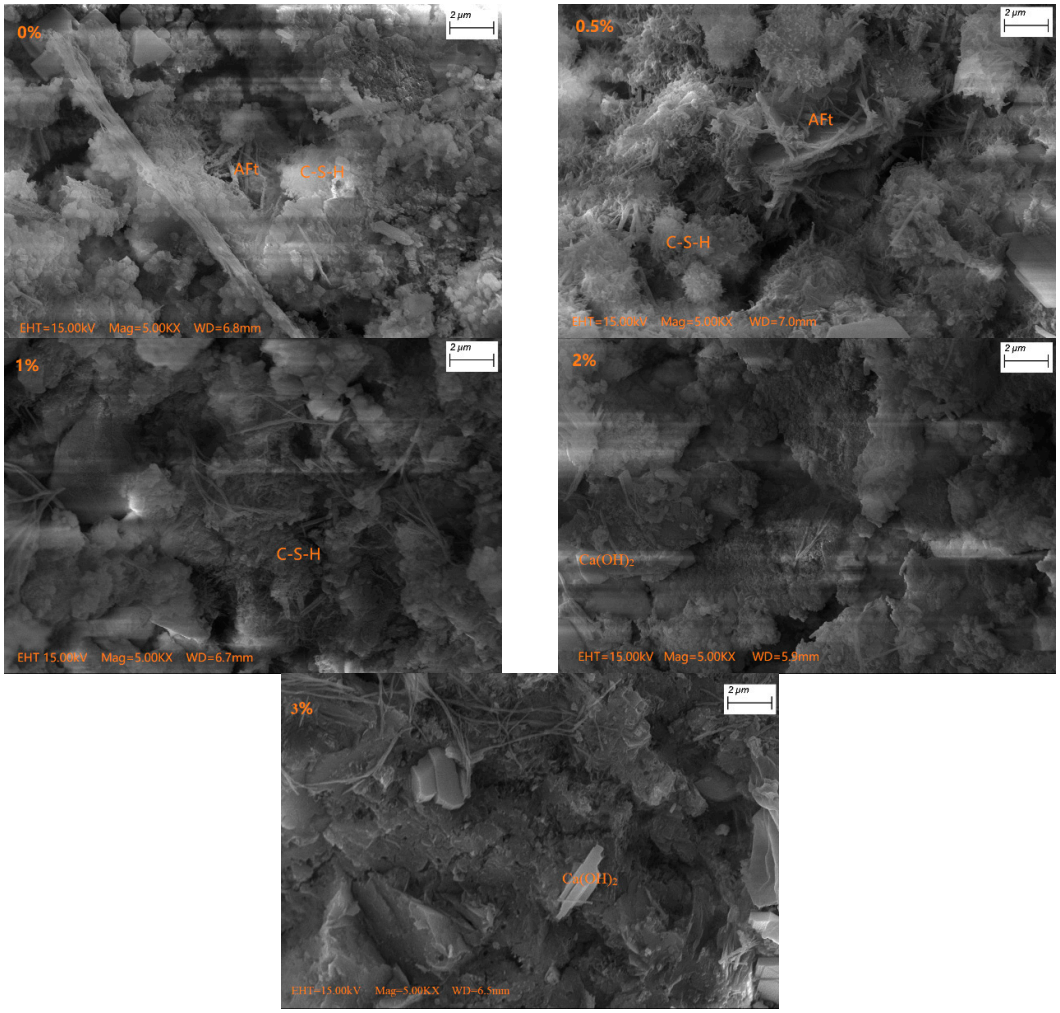

(**a**) 1 d.

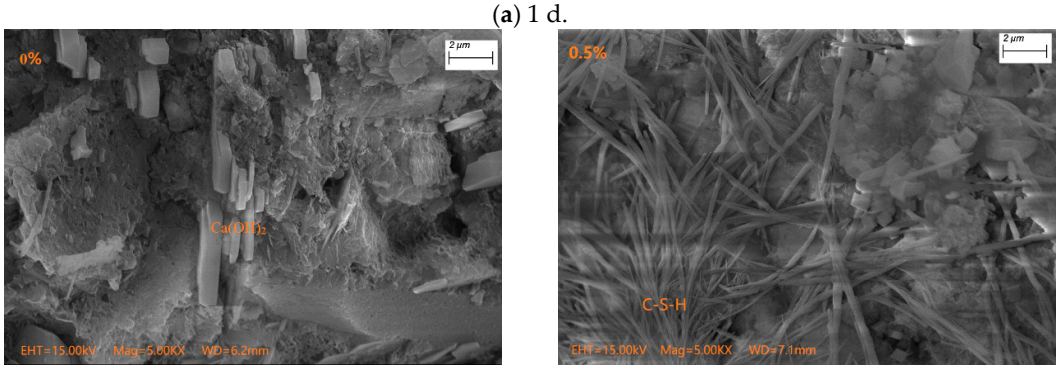

Figure 9. *Cont.*

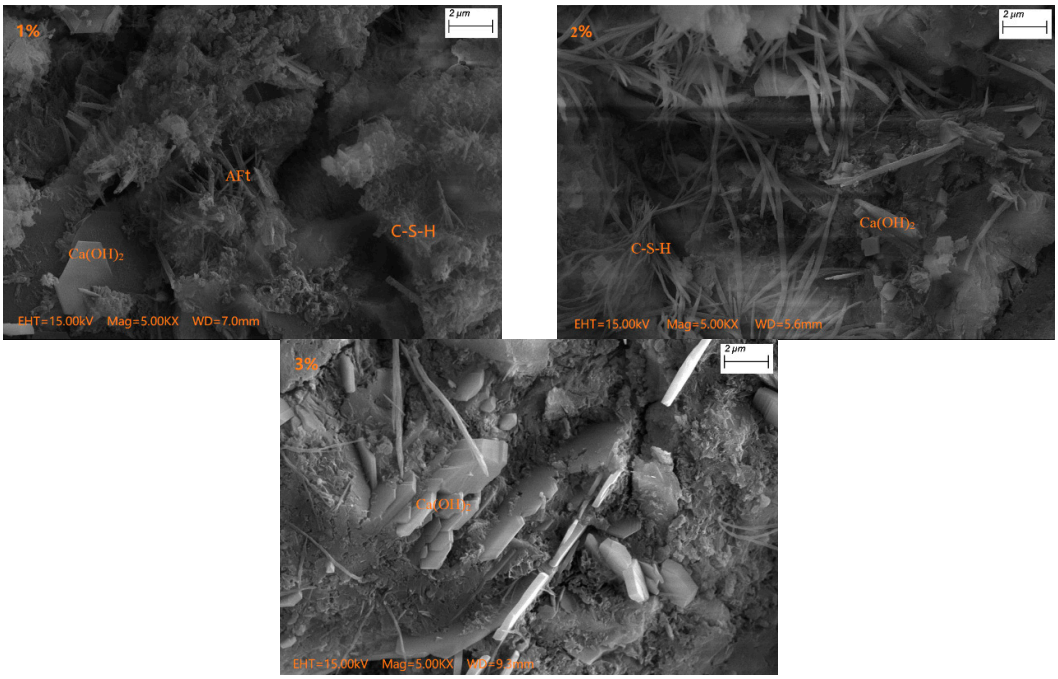

(**b**) 7 d.

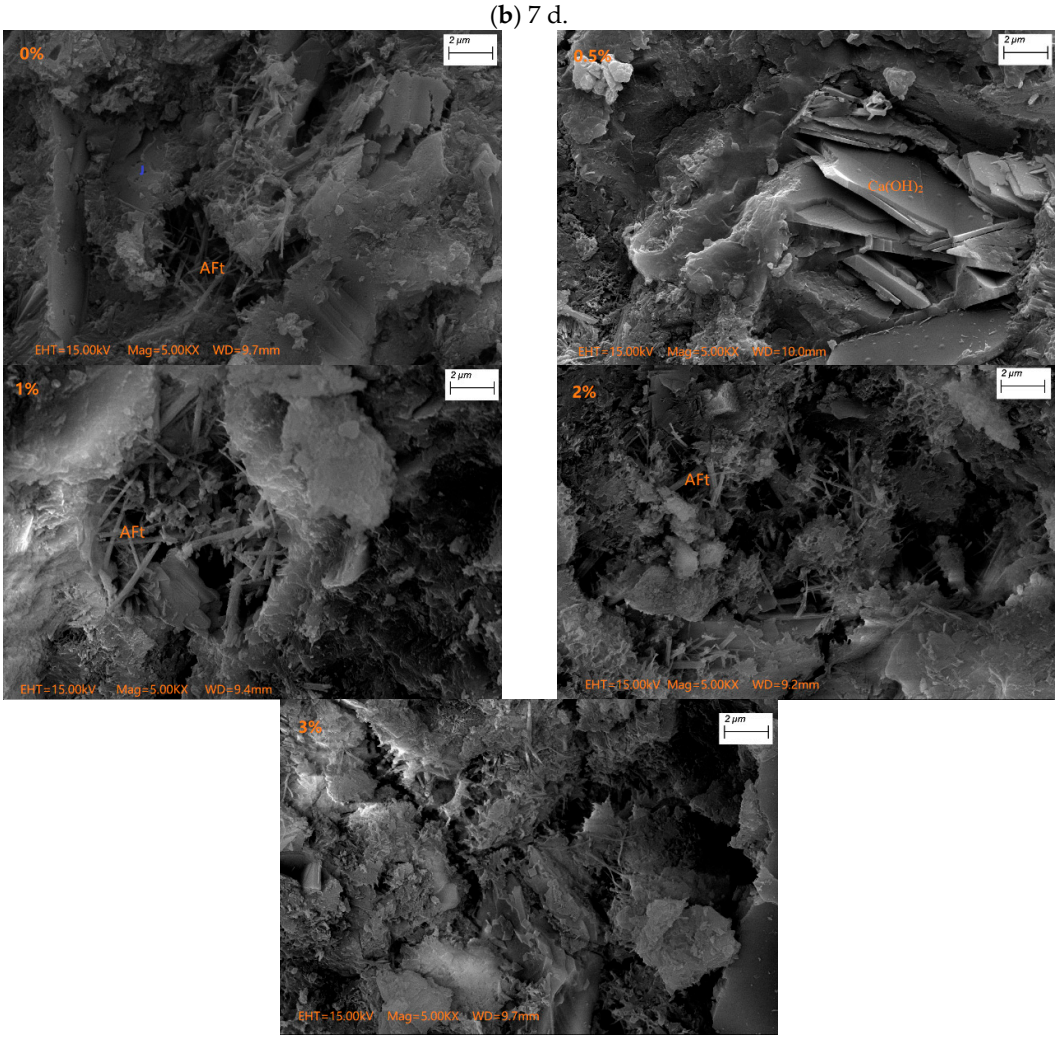

(**c**) 28 d.

Figure 9. SEM images of cement pastes with different contents of nano C-S-H particles at the age of 1, 7, and 28 days.

4. Conclusions

This study investigated the effect of synthesized highly crystalized nano C-S-H particles on the hydration of Portland cement paste. The setting time and compressive strength of different mixes with 0%, 0.5%, 1%, 2%, and 3% synthesized C-S-H particles are reported and discussed. The related mechanisms were analyzed through hydration heat, XRD, TG-DTA, and SEM tests. From the above results and analysis, the following conclusions can be drawn:

(1) Similar to the amorphous C-S-H particles, the synthesized high crystalized nano C-S-H particles could be used as an early strength agent for ordinary Portland cement, but the long-term performance still needs further investigation. The final setting time can be shortened by up to 30% and the 1-day compressive strength can be increased by 43% with the addition of 3% nano C-S-H particles.

(2) Although the addition of synthesized nano C-S-H particles could increase the early age strength (especially the 1-day strength), the later age strength (28 days) was decreased compared to that with no synthesized nano C-S-H particles. The reason could be that the initial accelerated hydration of cement caused by the addition of nano C-S-H particles did not form a compact structure, which was evidenced by the SEM observations.

(3) The mechanism of the effect of nano C-S-H particles on the ordinary Portland cement paste has been confirmed to be the accelerated hydration of C_3S and promoted formation of C-S-H gel and $Ca(OH)_2$ at early ages.

(4) In consideration of the results on both of the early age and later age strength development, 0.5%−1% synthesized nano C-S-H particles could be a suitable addition content in ordinary Portland cement. Compared to the cement paste with no addition of C-S-H particles, the final setting time can be shortened by 13%, while the compressive strength at the age of 1 and 7 days can be increased by 7% and 11%, respectively.

Author Contributions: Conceptualization, J.W. and Y.W.; methodology, J.W. and Y.W.; formal analysis, Y.W., H.H. and H.L.; investigation, H.L. and H.H.; writing—original draft preparation, H.L., J.W. and Y.W.; writing—review and editing, J.W. and Y.W.; supervision, J.W. and Y.W.; project administration, J.W. and Y.W.; funding acquisition, Y.W. All authors have read and agree to the published version of the manuscript.

Funding: This research was funded by National Natural Science Foundation of China (U1904188, 51678220), the Program for Innovation Scientists and Technicians Troop Construction Projects of Henan Province in China (CXTD2017088) and the Program for Innovative Research Team (in Science and Technology) (19IRTSTHN027).

Acknowledgments: The authors want to express their gratitude towards the support from Department of Civil Engineering, Tsinghua University, China.

Conflicts of Interest: The authors declare no conflict of interest.

Data Availability: Data used to support the findings of this study are available from the corresponding author upon request.

References

1. Lee, T.; Lee, J.; Choi, H.; Lee, D.-E. The Effects of fineness and TEA-based chemical admixture on early strength development of concrete in construction site application. *Materials* **2020**, *13*, 2027. [CrossRef]
2. Wang, S.D.; Liu, B.; Zhao, P.; Lu, L.; Cheng, X. Effect of early-strength-enhancing agents on setting time and early mechanical strength of belite-barium calcium sulfoaluminate cement. *J. Therm. Anal. Calorim.* **2018**, *131*, 2337–2343. [CrossRef]
3. Nguyen, H.-A.; Chang, T.-P.; Thymotie, A. Enhancement of early engineering characteristics of modified slag cement paste with alkali silicate and sulfate. *Const. Build. Mater.* **2020**, *230*, 117013. [CrossRef]
4. Carballosa, P.; Calvo, J.L.G.; Revuelta, D. Influence of expansive calcium sulfoaluminate agent on dosage on properties and microstructure of expansive self-compacting concretes. *Cem. Concr. Compos* **2020**, *107*, 103464. [CrossRef]
5. Heesup, C.; Masumi, I.; Hyeonggil, C. Physicochemical study on the strength development characteristics of cold weather concrete using a nitrite-nitrate based accelerator. *Materials* **2019**, *12*, 2706.

6. Sotiriadis, K.; Hikolopoulou, E.; Tsivilis, S.; Pavlou, A.; Chaniotakis, E.; Swamy, R.N. The effect of chlorides on the thaumasite form of sulfate attack of limestone cement concrete containing mineral admixtures at low temperature. *Constr. Build. Mater.* **2013**, *43*, 156–164. [CrossRef]
7. Wang, J. Steady-state chloride diffusion coefficient and chloride migration coefficient of cracks in concrete. *J. Mater. Civ. Eng.* **2017**, *29*, 0417117. [CrossRef]
8. Wang, J.; Basheer, P.A.M.; Nanukuttan, S.V.; Long, A.E.; Bai, Y. Influence of service loading and the resulting micro-cracks on chloride resistance of concrete. *Constr. Build. Mater* **2016**, *108*, 56–66. [CrossRef]
9. Wang, J.; Liu, E.; Li, L. Multiscale investigations on hydration mechanisms in seawater OPC paste. *Constr. Build. Mater.* **2018**, *191*, 891–903. [CrossRef]
10. Wang, J.; Liu, E. The relationship between steady-state chloride diffusion and migration coefficients in cementitious materials. *Mag. Concr. Res.* **2019**, *72*, 1016–1026, Ahead of print. [CrossRef]
11. Drolet, C.; Duchesne, J.; Fournier, B. Effect of alkali release by aggregates on alkali-silica reaction. *Constr. Build. Mater.* **2017**, *157*, 263–276. [CrossRef]
12. Ma, B.; Xu, Y.; Dong, R. Influence of Triethanolmine on the Initial Structure Formation and Mechanical Properties of Cement. *J. Build. Mater.* **2006**, *9*, 6–9.
13. Jiang, M.F.; Lü, X.J. Research and Application Progresses of Concrete Early Strength Agent. *J. Chin. Ceram. Soc.* **2014**, *33*, 2527–2533.
14. Ding, Z.; Xu, M.R.; Dai, J.G.; Dong, B.Q.; Zhang, M.J.; Hong, S.X.; Xing, F. Strengthening concrete using phosphate cement-based fiber-reinforced inorganic composites for improved fire resistance. *Constr. Build. Mater.* **2019**, *212*, 755–764. [CrossRef]
15. Xiao, L.; Zhang, H. Influence of New Composite Early Strength Agent on Mechanical Properties of Concrete (Mortar) and Its Mechanism Analysis. *B Chin. Ceram. Soc.* **2018**, *37*, 2115–2119.
16. El-Gamal, S.M.A.; Abo-El-Enein, S.A.; El-Hosiny, F.I.; Amin, M.S.; Ramadan, M. Thermal resistance, microstructure and mechanical properties of type I Portland cement pastes containing low-cost nanoparticles. *J. Therm. Anal. Calorim* **2018**, *131*, 949–968. [CrossRef]
17. Jo, B.W.; Kim, C.H.; Tae, G. Characteristics of cement mortar with nano-SiO2 particles. *Constr. Build. Mater* **2007**, *21*, 1351–1355. [CrossRef]
18. Najigivi, A.; Khaloo, A.; Zad, I.A.; Rashid, S.A. Investigating the effects of using different types of SiO_2 nanoparticles on the mechanical properties of binary blended concrete. *Compos. Part B Eng.* **2015**, *54*, 52–58. [CrossRef]
19. Zhao, Z.; Qi, T.; Zhou, W.; Hui, D.; Xiao, C.; Qi, J.; Zheng, Z.; Zhao, Z. A review on the properties, reinforcing effects, and commercialization of nanomaterials for cement-based materials. *Nanotechnol. Rev.* **2020**, *9*, 303–322. [CrossRef]
20. Shaikh, F.U.A.; Supit, S.W.M. Mechanical and durability properties of high volume fly ash (HVFA) concrete containing calcium carbonate ($CaCO_3$) nanoparticles. *Constr. Build. Mater.* **2014**, *70*, 309–321. [CrossRef]
21. Wang, J.; Liu, E.; Li, L. Characterization on the recycling of waste seashells with Portland cement towards sustainable cementitious materials. *J. Clean. Prod.* **2019**, *220*, 235–252. [CrossRef]
22. Praveenkumar, T.R.; Vijayalakshmi, M.M.; Meddah, M.S. Strengths and durability performances of blended cement concrete with TiO2 nanoparticles and rice husk ash. *Constr. Build. Mater.* **2019**, *217*, 343–351. [CrossRef]
23. Liu, Y.; Jia, M.; Song, C.; Lu, S.; Wang, H.; Zhang, G.; Yang, Y. Enhancing ultra-early strength of sulphoaluminate cement-based materials by incorporating graphene oxide. *Nanotechnol. Rev.* **2020**, *9*, 17–27. [CrossRef]
24. Wang, J.; Xu, Y.; Wu, X.; Zhang, P.; Hu, S. Advances of graphene- and graphene oxide- modified cementitious materials. *Nanotechnol. Rev.* **2020**, *9*, 465–477. [CrossRef]
25. Sun, J.; Xu, K.; Shi, C.; Ma, J.; Li, W.; Shen, X. Influence of core/shell TiO_2@SiO_2 nanoparticles on cement hydration. *Constr. Build. Mater.* **2017**, *156*, 114–122. [CrossRef]
26. El-Gamal, S.M.A.; El-Hosiny, F.I.; Amin, M.S.; Sayed, D.G. Ceramic waste as an efficient material for enhancing the fire resistance and mechanical properties of hardened Portland cement pastes. *Constr. Build. Mater.* **2017**, *154*, 1062–1078. [CrossRef]
27. Gao, Y.; Jing, H.; Du, M.; Chen, W. Dispersion of Multi-Walled Carbon Nanotubes Stabilized by Humic Acid in Sustainable Cement Composites. *Nanomaterials* **2018**, *8*, 858. [CrossRef]

28. Gao, Y.; Jing, H.; Zhou, Z. Fractal analysis of pore structures in graphene oxide-carbon nanotube based cementitious pastes under different ultrasonication. *Nanotechnol. Rev.* **2019**, *8*, 107–115. [CrossRef]
29. Gao, Y.; Jing, H.W.; Chen, S.J.; Du, M.R.; Chen, W.Q.; Duan, W. Influence of ultrasonication on the dispersion and enhancing effect of graphene oxide–carbon nanotube hybrid nanoreinforcement in cementitious composite. *Compos. Part B Eng.* **2019**, *164*, 45–53. [CrossRef]
30. Konsta-Gdoutos, M.S.; Metaxa, Z.S.; Shahb, S.P. Highly dispersed carbon nanotube reinforced cement based materials. *Cem. Concr. Res.* **2010**, *40*, 1052–1059. [CrossRef]
31. Li, G.Y.; Wang, P.M.; Zhao, X. Mechanical behavior and microstructure of cement composites incorporating surface-treated multi-walled carbon nanotubes. *Carbon* **2005**, *43*, 1239–1245. [CrossRef]
32. Musso, S.; Tulliani, J.M.; Ferro, G.; Tagliaferro, A. Influence of carbon nanotubes structure on the mechanical behavior of cement composites. *Compos. Sci. Technol.* **2009**, *69*, 1985–1990. [CrossRef]
33. Wang, F.; Kong, X.; Jiang, L.; Wang, D. The acceleration mechanism of nano-C-S-H particles on OPC hydration. *Constr. Build. Mater.* **2020**, *249*, 118734. [CrossRef]
34. Zhang, C.Y.; Cai, Y.; Kong, X.M.; Hao, T.Y. Influence of Nano C-S-H on Cement Hydration, Pore Structure of Hardened Cement Pastes and Strength of Concrete. *J. Chin. Ceram. Soc.* **2019**, *47*, 585–593.
35. Jee, H.; Park, J.; Zalnezhad, E. Characterization of titanium nanotube reinforced cementitious composites: Mechanical properties, microstructure, and hydration. *Materials* **2019**, *12*, 1617. [CrossRef]
36. Zhuang, C.; Chen, Y. The effect of nano-SiO_2 on concrete properties: A review. *Nanotechnol. Rev.* **2019**, *8*, 562–572. [CrossRef]
37. Land, G.; Stephan, D. Controlling cement hydration with nanoparticles. *Cem. Concr. Compos.* **2015**, *57*, 64–67. [CrossRef]
38. Wang, F.; Kong, X.; Wang, D.; Wang, Q. The effects of nano-C-S-H with different polymer stabilizers on early cement hydration. *J. Am. Ceram. Soc.* **2019**, *102*, 5103–5116. [CrossRef]
39. Kong, D.; He, G.; Pan, H.; Weng, Y.; Du, N.; Sheng, J. Influences and mechanisms of nano-S-C-H gel addition on fresh properties of the cement-based materials with sucrose as retarder. *Materials* **2020**, *13*, 2345. [CrossRef]
40. Kanchanason, V.; Plank, J. Effect of calcium silicate hydrate—Polycarboxylate ether (C-S-H-PCE) nanocomposite as accelerating admixture on early strength enhancement of slag and calcined blended cements. *Cem. Concr. Res.* **2019**, *119*, 44–50. [CrossRef]
41. Das, S.; Ray, S.; Sarkar, S. Early strength development in concrete using preformed CSH nano crystals. *Constr. Build. Mater.* **2020**, *233*, 117214. [CrossRef]
42. Standardization Administration of the People's Republic of China. *GB175-2007: Common Portland Cement*; China Architecture and Building Press: Beijing, China, 2007.
43. He, Y.; Zhao, X.; Lu, L.; Struble, L.J.; Hu, S. Effect of C/S Ratio on Morphology and Structure of Hydrothermally Synthesized Calcium Silicate Hydrate. *J. Wuhan Univ. Technol. Mater. Sci. Ed.* **2011**, *26*, 770–773. [CrossRef]
44. Lei, Y.S.; Han, T.; Wang, H.Q.; Jin, X.Z.; Fang, Y.; Cao, H.H.; Cheng, F.Q. Preparation and characterization of calcium silicate hydrate(C-S-H) synthesized by the hydrothermal method. *Bull. Chin. Ceram. Soc.* **2014**, *33*, 465–469.
45. Richardson, I.G. The calcium silicate hydrates. *Cem. Concr. Res.* **2008**, *38*, 137–158. [CrossRef]
46. Taylor, H.F.W. Proposed structure for calcium silicate hydrate gel. *J. Am. Ceram. Soc.* **1986**, *69*, 464–467. [CrossRef]
47. China Academy of Building Research. *JGJ 63-2006: Standard of Water for Concrete*; China Architecture and Building Press: Beijing, China, 2006.
48. Standardization Administration of the People's Republic of China. *GB/T1346-2011: Test Methods for Water Requirement of Normal Consistency, Setting Time and Soundness of the Portland Cement*; China Architecture and Building Press: Beijing, China, 2011.
49. Standardization Administration of the People's Republic of China. *GB/T17671-1999: Method of Testing Cements-Determination of Strength*; The State Bureau of Quality and Technical Supervision: Beijing, China, 1999.
50. Wang, Y.; He, F.; Wang, J.; Wang, C.; Xiong, Z. Effects of calcium bicarbonate on the properties of ordinary Portland cement paste. *Constr. Build. Mater.* **2019**, *225*, 591–600. [CrossRef]
51. Wang, Q.; Li, S.Y.; Wang, J.; Pan, S.; Lv, C.X.; Cui, X.Y.; Guo, Z.W. Effect of Graphene Oxide on Hydration Process and Main Hydration Products of Cement. *J. Chin. Ceram. Soc.* **2018**, *46*, 163–172.
52. Thomas, J.J.; Jennings, H.M.; Chen, J.J. Influence of nucleation seeding on the hydration mechanisms of tricalcium silicate and cement. *J. Phys. Chem. C* **2009**, *113*, 4327–4334. [CrossRef]

53. Land, G.; Stephan, D. The effect of synthesis conditions on the efficiency of C-S-H seeds to accelerate cement hydration. *Cem. Concr. Compos.* **2018**, *87*, 73–78. [CrossRef]
54. Pedrosaa, H.C.; Realesb, O.M.; Reisb, V.D.; Maria das Dores Paivab, M.D.; Fairbairna, E.M.R. Hydration of Portland cement accelerated by C-S-H seeds at different Temperatures. *Cem. Concr. Res.* **2020**, *129*, 105978. [CrossRef]